

Evaluation of ponding analysis methods using 3-D finite element modelling

A. Schouten, J. Locht, J.P.B.N. Derks

Schouten Engineering Consultancy B.V. Breda, The Netherlands

Water accumulation is studied by application of the developed in-house software WACSIM, able to model the ponding behaviour of one-dimensional, two-dimensional and three-dimensional structures. All analyses are accomplished under the regime of the Dutch building code NEN 6702, the latest version of which requires, in a water accumulation analysis, a reduction of the structural stiffness data by a model factor γ_M , intended as an instrument to guarantee larger safety. The first part of the article reports statistics of a large number of cases, showing that a prescribed fixed value of the model factor yields a big scatter in the real safety. The second part of the article offers a comparison of the computational results with the outcome of the analytical results as published in this Heron edition. The third part of the article discloses the importance of a three-dimensional analysis in which the complete real roof structure is adequately modelled. Simplified computational schemes yield different failure modes than those occurring in a full three-dimensional model.

Key words: Ponding, flat roofs, accumulation of rainwater, steel, statistical evaluation, finite element analysis, analytical solution methods, comparison, case study

1 Introduction

For almost ten years flat roof structures have been analysed that are collapsed due to excessive ponding. From the start three-dimensional finite element models of the roof and its supporting structure were used. WACSIM (Water ACcumulation SIMulation) is the in-house developed software for generating the ponding loads on the roof model. Over the last years the goal of the calculations shifts from failure analysis to preventive analysis leading to an advice for the emergency drainage system to be installed.

Besides the numerical analysis, also available analytical solutions have been studied and their usefulness in an engineering environment was assessed. This leads to the following observations.

- Analytical solutions presented in literature sometimes neglect self-weight and thus only consider the ponding loads. However, this is an oversimplification of reality, and in such cases the presented solutions are more academic exercises than useful and fruitful methods for designing engineers.
- Analytical methods can only be developed for regular roof plans of orthogonal pattern. The ponding stability behaviour is different for each structure, which implies a strong path-dependency, which could most probably only be traced by numerical analysis. As a consequence the validity of analytical solution methods is rather limited.
- In order to avoid unsafe situations it should be underlined that the analytical solution methods lose their applicability for $n < 1$ due to the nonlinear stability response. Only very recently a theory was published to overcome this restriction (Blaauwendraad, 2007, Engineering Structures).

Noteworthy is that this article highlights key issues related to the solution of ponding (nonlinear load) problems and consequently phenomena like geometrical nonlinearities and physical nonlinearities are not covered. Although it is easy to incorporate these effects in the ponding analysis, the interested readers may care to consult literature (e.g. the publication of Colombi 2006) for an extensive discussion and exhaustive treatment of these kinds of problems and associated topics.

The statistical information of the many ponding analyses performed over the years is discussed in the next chapter. Chapter 3 presents a comparison of the WACSIM software with analytical models. Chapter 4 discusses a typical case study, demonstrating the benefit or rather necessity of 3-D finite element ponding analysis.

In this article all safety requirements are drawn from the Dutch building code NEN 6702. This code was drafted in 1991, adapted in 1997 and revised in 2001. Hereafter, these code editions will be called 'old'. In 2006 the code was adapted again with respect to water accumulation. The model factor γ_M was introduced by which all stiffness data of a structure must be divided. *This factor is supposed* to rule out the situation that the prescribed water level lies just below the stability dictated water depository capacity in case of ponding. Hereafter, this revised code will be called the 'new' code edition. As a consequence of the model factor, larger than 1,0, the water accumulation will be exaggerated, and an additional safety margin to the actual failure water elevation is obtained.

2 Statistical evaluation

A statistical evaluation of approximately 200 *in-house* analysed roofs regarding ponding sensitivity supported the following findings.

- Only 3% of the analysed roofs comply with the old Dutch Code Regulations regarding ponding.
- Approximately 14% shall not collapse for the specified initial water elevation but do not meet completely the safety levels of the Dutch Code Regulations.
- 57% will survive when regular drainage is operational, but these shall most likely collapse due to severe rainfall in case the regular water discharge drains are blocked.
- 26% are extremely sensitive for ponding and the risk of collapse is high in the case of rainfall.

The outcome of recently executed *external* investigations and studies (report of VROM 2003) concerning 100 ponding collapse cases demonstrates that none of the examined roofs did meet the Dutch Code Requirements. This emphasizes the statement in the VROM publication that the old Code NEN 6702 was sound and fit for purpose.

Now the impact of the introduction of the model factor γ_M for stiffness reduction will be studied. A set of 17 structures - a good mix of structures as will occur in practice - is analysed in different ways to assess the consequences of γ_M for the safety of roofs. Firstly the definitions, notions and assumptions are briefly summarized to explain which analyses have been made. Secondly a representative quantitative data set retrieved from the *in-house* executed ponding assessments is introduced in table format.

- Initial water elevation h_{ini} : is the initial water elevation measured with respect to the lowest point on the considered roof surface.
- Initial water elevation $h_{ini,collapse}$: is the initial water elevation when *collapse* occurs. This water elevation is calculated with load factors 1,0 for both dead load and live load (water), and without application of any model factor for stiffness reduction.
- Initial water elevation $h_{ini,allowed;\gamma_M=1}$: is the *allowable* initial water elevation according to the *old* Dutch Code NEN 6702 (model factor $\gamma_M = 1,0$) with the demanded safety. This water elevation is calculated with load factors 1,2 for dead load and 1,5 for water load.

- Initial water evaluation $h_{ini,allowed; \gamma_M=1,1}$: is the *allowable* initial water elevation according to the *new* Dutch Code NEN 6702 (model factor $\gamma_M = 1,1$) with the demanded safety. This water elevation is calculated with load factors 1,2 for dead load and 1,5 for water load.
- Initial water evaluation $h_{ini,allowed; \gamma_M=1,3}$: is the *allowable* initial water elevation according to the *new* Dutch Code NEN 6702 (model factor $\gamma_M = 1,3$) with the demanded safety. This water elevation is calculated with load factors 1,2 for dead load and 1,5 for water.
- The safety factor $SF_{NEN\ 6702; \gamma_M=1} = h_{ini,collapse} / h_{ini,allowed; \gamma_M=1}$
- The safety factor $SF_{NEN\ 6702; \gamma_M=1,1} = h_{ini,collapse} / h_{ini,allowed; \gamma_M=1,1}$
- The safety factor $SF_{NEN\ 6702; \gamma_M=1,3} = h_{ini,collapse} / h_{ini,allowed; \gamma_M=1,3}$
- The adopted increment/decrement size is 5 mm for computation of the initial water elevation.

Table 1: Overview of initial water elevations in mm for model factor $\gamma_M = 1,0 / 1,1 / 1,3$

| Object | $h_{ini,collapse}$ | $h_{ini,allowed; \gamma_M=1}$ | $h_{ini,allowed; \gamma_M=1,1}$ | $h_{ini,allowed; \gamma_M=1,3}$ |
|--------|--------------------|-------------------------------|---------------------------------|---------------------------------|
| 1 | 100 | 70 | 70 | 65 |
| 2 | 100 | 65 | 60 | 50 |
| 3 | 160 | 120 | 115 | 110 |
| 4 | 45 | 15 | 15 | 10 |
| 5 | 85 | 65 | 55 | 40 |
| 6 | 85 | 70 | 60 | 45 |
| 7 | 185 | 130 | 130 | 120 |
| 8 | 130 | 110 | 95 | 75 |
| 9 | 65 | 50 | 40 | 30 |
| 10 | 100 | 85 | 75 | 55 |
| 11 | 135 | 115 | 110 | 100 |
| 12 | 160 | 120 | 120 | 110 |
| 13 | 70 | 40 | 35 | 10 |
| 14 | 100 | 65 | 55 | 40 |
| 15 | 85 | 55 | 50 | 35 |
| 16 | 75 | 55 | 50 | 40 |
| 17 | 155 | 90 | 85 | 75 |

- The investigated structures (objects) belong all to safety class 3 with corresponding load factors in the Ultimate Limit State: $\gamma_{f;g;u} = 1,2$ and $\gamma_{f;q;u} = 1,5$ for dead load and water load respectively; (The notation of the Dutch code is followed).
- The applied gravitational acceleration is $9,81 \text{ m/s}^2$.

The numerically obtained data set is collected in the Tables 1-2. It can be observed that the scatter of the safety factor is disproportionate and incalculable for model factor $\gamma_M = 1,3$. This behavior is also tangible for model factor $\gamma_M = 1,1$.

A reasonable engineering *estimate* for the required safety is given in order to provide some guidance for judgement of the listed results by the reader. It is required to compute the Fundamental Load Combination in the Ultimate Limit State for safety class 3 according to:
 $\gamma_{f;g;u} \cdot \text{Dead load} + \gamma_{f;q;u} \cdot \text{Live load} = 1,2 \cdot \text{Dead load} + 1,5 \cdot \text{Live load} (\text{p}_{\text{rep;water}})$.

Table 2: Summary of safety factors with respect to collapse for model factor $\gamma_M = 1,0 / 1,1 / 1,3$

| Object | SF _{NEN 6702;$\gamma_M=1$} | SF _{NEN 6702;$\gamma_M=1,1$} | SF _{NEN 6702;$\gamma_M=1,3$} |
|--------|--|--|--|
| 1 | 1,43 | 1,43 | 1,54 |
| 2 | 1,54 | 1,67 | 2,00 |
| 3 | 1,33 | 1,39 | 1,45 |
| 4 | 3,00 | 3,00 | 4,50 |
| 5 | 1,31 | 1,55 | 2,13 |
| 6 | 1,21 | 1,42 | 1,89 |
| 7 | 1,42 | 1,42 | 1,54 |
| 8 | 1,18 | 1,37 | 1,73 |
| 9 | 1,30 | 1,63 | 2,17 |
| 10 | 1,18 | 1,33 | 1,82 |
| 11 | 1,17 | 1,23 | 1,35 |
| 12 | 1,33 | 1,33 | 1,45 |
| 13 | 1,75 | 2,00 | 7,00 |
| 14 | 1,54 | 1,82 | 2,50 |
| 15 | 1,55 | 1,70 | 2,43 |
| 16 | 1,36 | 1,50 | 1,88 |
| 17 | 1,72 | 1,82 | 2,07 |

Assuming that the Dead load equals the Live (Ponding) load, and both having value 1,0, the following relationship holds:

$$SF_{\text{averaged estimate}} = \frac{\gamma_{f,g,w} \cdot \text{Dead load} + \gamma_{f,q,w} \cdot \text{Live load}}{\text{Dead load} + \text{Live load}} = \frac{1,2 \cdot 1,0 + 1,5 \cdot 1,0}{2,0} = 1,35$$

Naturally, the required safety should have a value between 1,2 and 1,5. Of course, higher safety values are yet possible, but those are not requested.

For ease of survey the results are reprocessed in Figure 1.

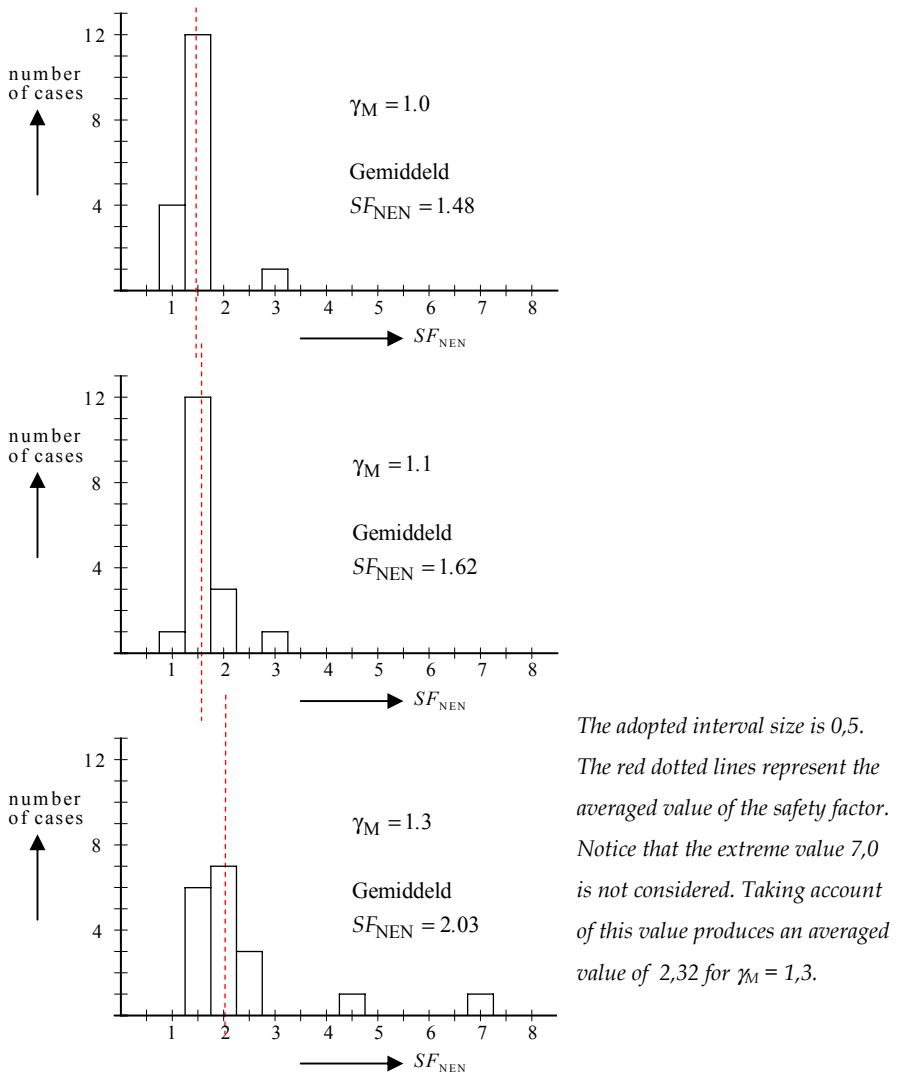


Figure 1: Number of cases versus safety factor for model factor $\gamma_M = 1,0 / 1,1 / 1,3$

The graphs show transparently that for model factor $\gamma_M = 1,0$ the averaged computed safety factor is already in the defined range. Accordingly, the model factor $\gamma_M = 1,3$ raises the averaged safety factor needless for certain cases.

3 Comparison of results for a two-way roof system

Analytical solutions are available for a two-way flat roof system, i.e. with primary and secondary members (Marino 1966; Herwijnen et al 2007; Blaauwendraad 2007, Engineering Structures). Results of the 3-D numerical software are compared with an analytical example calculation. Here we choose the analytical methods of Herwijnen et al and Blaauwendraad, which are included in this edition of Heron. It must be kept in mind that the model of Herwijnen et al starts from negligible deformation of the roof plates. The Blaauwendraad model can be applied in two ways, either neglecting the roof plate deformation or accounting for it, and the Schouten software is able to include the deformation of the roof plates.

3.1 Example

The input parameters for the example flat roof structure are:

- Span of primary member (beam) 20 m
- Span of secondary member (girder) 10 m
- Distance between secondary members 5 m
- Profile of primary member HEA 800
- Profile of secondary member IPE 400
- Roof plates (sheeting) SAB 100R/825, $t_N = 0,75$ mm
- Permanent load $0,2$ kN/m², including roof plates
- Gravitational acceleration 10 m/s²
- Initial water level 150 mm
- Safety class 2: safety factors in the Ultimate Limit State: $\gamma_{f;g,u} = 1,2$ and $\gamma_{f;q,u} = 1,3$

The beams are simply supported on rigid supports. The girders are flexibly supported by the beams and the connection with the beam is by a simple support. The following modelling assumption is adopted for the roof plates (sheeting): the sheeting continues over the girders (1 x 4-field span).

3.2 *Finite Element Model*

The finite element model utilizes a surface to apply the hydrostatic loads on. Therefore shell elements representing roof sheeting are selected. The modelled stiffness is based on the properties of realistic roof slabs. This provides us the opportunity to investigate the influence of the roof sheeting, which is normally neglected in analytical solutions for ponding. As far as known, only Blaauwendraad attempts to include the effect of sheeting on ponding (Blaauwendraad 2007, Engineering Structures). Beam elements represent the underlying steel structure. The girders are simply supported by the main beam, which means they are connected by *hinges*. The roof plates are modelled with orthotropic shell elements.

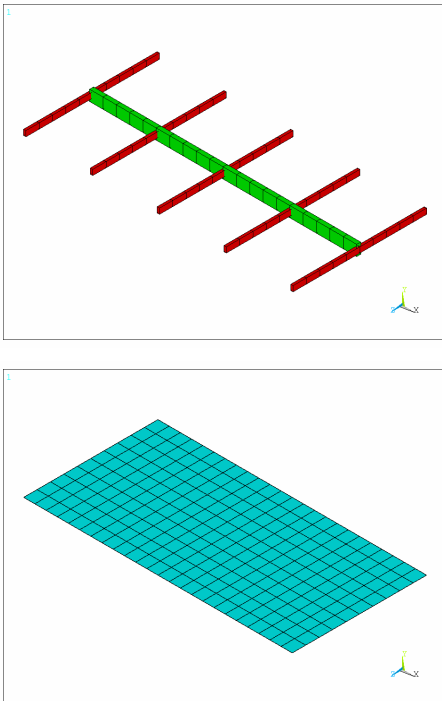


Figure 2: Beam elements represent primary and secondary members; flat shell elements represent roof plating

3.3 *Comparison*

The outcome of the analytical and finite element ponding analyses are given for two defined cases.

- Case 1. Sheeting deflection not considered
- Case 2. Sheeting deflection considered (roof: 1 x 4-field span)

Results of the analytical and finite element ponding analysis cases are compared in the tables below, for deflections and stresses respectively. The results for the analytical model of Herwijnen et al are taken from this Heron issue. The results of the Blaauwendraad closed-form model were obtained by application of his theory (Blaauwendraad, 2007, Engineering Structures). The relative deviation of the analytical results compared to the WACSIM results are also listed in the tables below.

3.3.1 Results sheeting deflection not considered

It should be underscored that the stiffness of the steel sheeting in the finite element model is increased, i.e. shell element deflection is reduced. As a result the effect of the roof flexibility is limited in order to acquire a sound comparison. Comparison of the results points to that the scatter is relative small.

Table 3: Calculated deflections due to Dead load

| Method | Beam | Girder | Sheeting | Unit |
|--------------------|---------|---------|----------|------|
| Blaauwendraad | 18 | 4,5 | - | mm |
| Herwijnen | 18 | 4,5 | - | mm |
| WACSIM | 17 | 4,3 | - | mm |
| Relative deviation | +5%/+5% | +5%/+5% | - | - |

Table 4: Calculated deflections caused by Dead load and Live load ($h_{mi} = 150$ mm)

| Method | Beam | Girder | Sheeting | Unit |
|--------------------|----------|----------|----------|------|
| Blaauwendraad | 104 | 40 | - | mm |
| Herwijnen | 100 | 43 | - | mm |
| WACSIM | 94 | 38 | - | mm |
| Relative deviation | +10%/+6% | +5%/+13% | - | - |

Table 5: Calculated stresses caused by Dead load and Live load ($h_{ini} = 150 \text{ mm}$) in the Ultimate Limit State

| Method | Beam | Girder | Sheeting | Unit |
|--------------------|---------|----------|----------|-------------------|
| Blaauwendraad | 268 | 208 | - | N/mm ² |
| Herwijnen | 262 | 226 | - | N/mm ² |
| WACSIM | 251 | 201 | - | N/mm ² |
| Relative deviation | +6%/+4% | +3%/+12% | - | - |

3.3.2 Results sheeting deflection considered

(sheeting continuously supported by girders: 1 x 4-field span)

In this case the roof plates are idealized according to reality, that is, SAB 100R/825. The model results of Blaauwendraad and WACSIM are compared. Comparison of the deflection results indicates that the Blaauwendraad model deviates, however the differences in the stress values are relative small. No further explanation is given. A general remark is that analytical models are valuable, but they should be carefully applied.

Table 6: Calculated deflections due to Dead load

| Method | Beam | Girder | Sheeting | Unit |
|--------------------|------|--------|----------|------|
| Blaauwendraad | 18 | 5 | 5 | mm |
| WACSIM | 18 | 5 | 5* | mm |
| Relative deviation | 0% | 0% | 0% | - |

This value is varying due to the position dependency

Table 7: Calculated deflections caused by Dead load and Live load ($h_{ini} = 150 \text{ mm}$)

| Method | Beam | Girder | Sheeting | Unit |
|--------------------|------|--------|----------|------|
| Blaauwendraad | 114 | 49 | 20 | mm |
| WACSIM | 101 | 40 | 29* | mm |
| Relative deviation | +12% | +22% | -32% | - |

This value is varying due to the position dependency

Table 8: Calculated stresses caused by Dead load and Live load ($h_{ini} = 150 \text{ mm}$) in the Ultimate Limit State

| Method | Beam | Girder | Sheeting | Unit |
|--------------------|------|--------|----------|-------------------|
| Blaauwendraad | 291 | 227 | 424 | N/mm ² |
| WACSIM | 270 | 214 | 439 | N/mm ² |
| Relative deviation | +7% | +6% | -4% | - |

4 Importance of 3-D Ponding Check of Structure (application)

A salient practical example of a 3-D Finite Element ponding analysis is elucidated. Schouten Engineering Consultancy B.V. was hired for execution and evaluation of the numerical ponding check of the critical roof structure and examination of the present installed emergency water discharge drains both according to the valid Dutch Code regulations. For this purpose numerical calculations were performed by application of finite element software. The loads are identified and selected according to the Dutch Code NEN 6702 (TGB 1990) and the supplied project data.

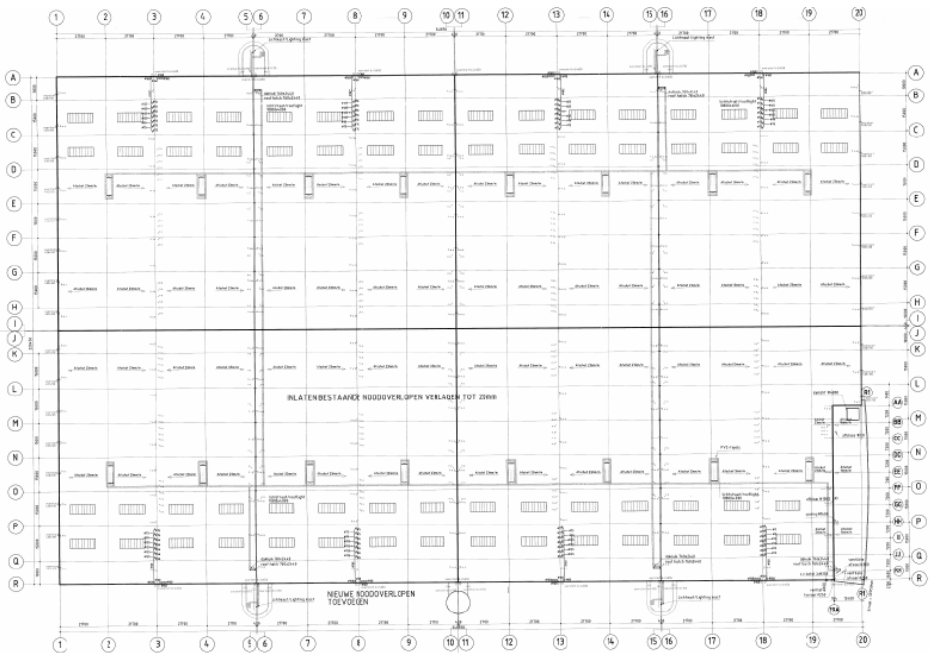


Figure 3: Plan of structure

In this article attention is confined to the numerical ponding check.

The analysis will be done with three different computational models, called 2-D, 2½-D and 3-D analysis. The purpose is to investigate if, and if yes to which extent, these approaches yield reliable results. It is told beforehand that the reader is referred to Section 4.1 for an overview of the structure and Section 4.2 for a brief exposition of the models.

4.1 Geometry of Structure

The roof structure is a 3-way structure composed of trusses (primary members), girders (secondary members) and profiled steel sheeting (roof slabs, tertiary members) supported by columns, façades. The object geometry is schematically displayed in Figures 3-5.

4.2 Outline of Finite Element Model

The employed finite element geometry is displayed in Figures 6-7. Trusses, girders and columns are modelled by 3-D beam elements with tension, compression, torsion, and bending capabilities. The roof sheeting is idealized by orthotropic shell elements which have both bending and membrane capabilities. Both in-plane and normal loads are permitted. Orthotropic material directions correspond to the element coordinate directions. Data on stiffness and strength are skipped here, taking into account the primary goal of the analyses to show the difference in failure mode for different perfection (abstraction) levels of computational models. The beam camber (secondary members) and initial slope (23 mm per meter for primary members and tertiary members) are modelled.

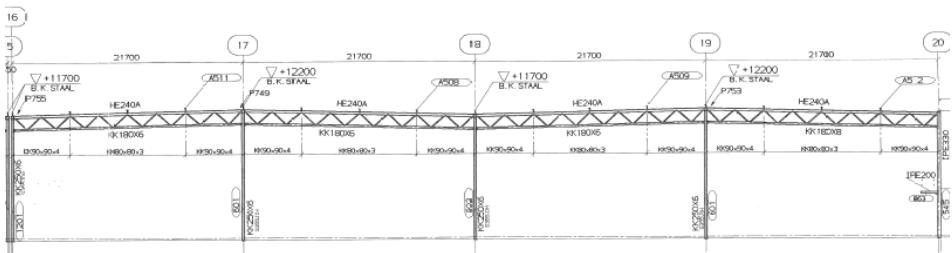


Figure 4: Layout of trusses (primary members)



Figure 5: Outline of girders (secondary members)

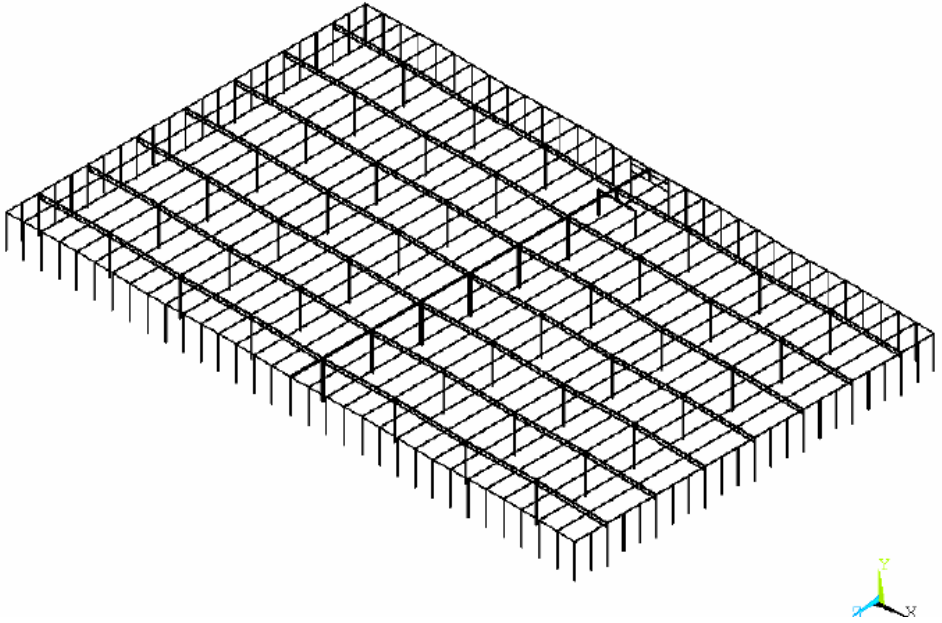
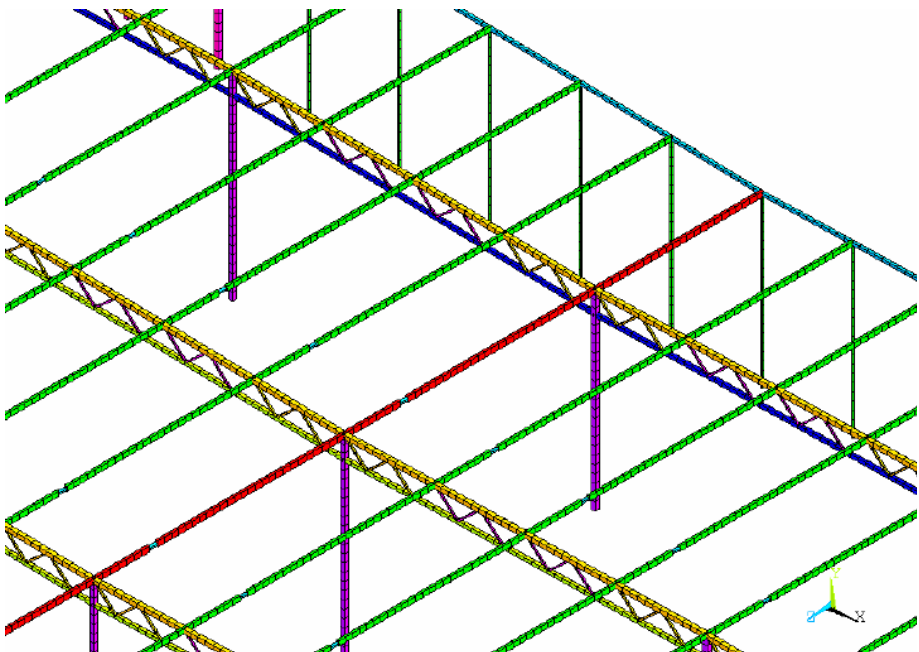


Figure 6: View of the trusses (primary members), girders (secondary members) and columns



Structural composition of steel columns, steel trusses and steel girders (red indicated is the IPE 300 girder)

Figure 7: Zoom of the structural steel work (trusses/girders/columns)

The initial slope is difficult to idealize with 2-D or 2½-D numerical models. The 2½-D model represents a slice of the structure, which includes the main girder (IPE 300), the adjacent girders (IPE 270) and steel sheeting. The 2-D model includes the slope, but deflection of the roof plating is not considered. The 2-D model covers the main girder, while the influence of the adjacent girders is incorporated through analytical formulae. Both 2-D model and 2½-D model are supplemented with a small initial imperfection.

4.3 Strength Criteria

4.3.1 Ponding (TGB 1990)

The roof structure must be analyzed, evaluated and computed for the ponding case according to the paragraph 8.7.1.2 of the Dutch Code NEN 6702.

It is tacitly assumed that water transport through the regular water discharge drains is not possible. The water transfer above the roof edge and through the emergency water discharge drains is yet possible and this restriction is used for the calculation of the initial water height.

4.3.2 Fundamental Load Combination in the Ultimate Limit State: Dead Load and Live Load (ponding) (TGB 1990)

The object is categorized in safety class 2, i.e.,

$$\gamma_{f;g,u} \cdot \text{Dead load} + \gamma_{f;q,u} \cdot \text{Live load} = 1,2 \cdot \text{Dead load} + 1,3 \cdot \text{Live load (p}_{\text{rep,water}}).$$

4.4 Numerical Results

The deflection modes are visualized for three water elevation heights (h_{ini}) in order to show the typical response of the aforementioned 2-D, 2½-D and 3-D finite element models. The results are supplied for the governing IPE 300 girder and are depicted in the figures addressed below. The numerically computed deflection modes for $h_{ini} = 42$ mm are presented in the figures 8-10. It is clearly visible that the response of the three models is conformal for this water elevation, which indicates that all three model approaches are valid.

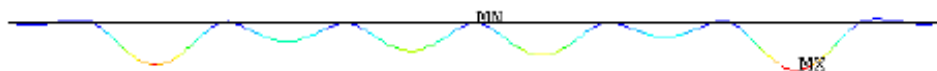


Figure 8: Plot of deflections IPE 300 girder 2-D model $h_{ini} = 42$ mm. Maximum value 51,57 mm

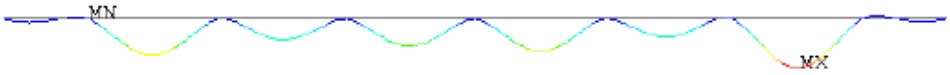


Figure 9: Plot of deflections IPE 300 girder 2½-D model $h_{ini} = 42$ mm. Maximum value 39,61 mm

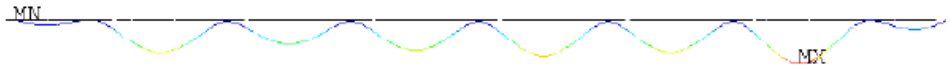


Figure 10: Plot of deflections IPE 300 girder 3-D model $h_{ini} = 42$ mm. Maximum value 52,38 mm

The numerically determined deflection modes for $h_{ini} = 65$ mm are devised in the figures beneath. It can be seen that the 2D-model lost its validity, namely the 2-D and 3-D displacement fields resembles huge deviations. Furthermore, it can be observed that the 2½-D model starts gradually losing its legitimacy. Besides that, it can be expected that also the 2½-D model shall lose its applicability when the water elevation exceeds a certain threshold value.

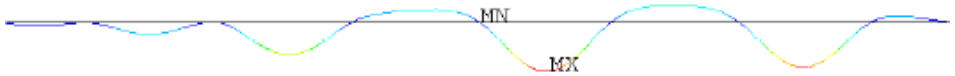


Figure 11: Plot of deflections IPE 300 girder 2-D model $h_{ini} = 65$ mm. Maximum value 128,97 mm



Figure 12: Plot of deflections IPE 300 girder 2½-D model $h_{ini} = 65$ mm. Maximum value 80,27 mm

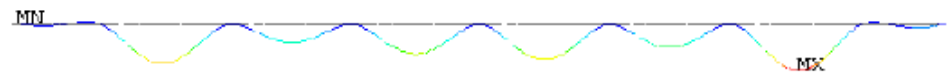


Figure 13: Plot of deflections IPE 300 girder 3-D model $h_{ini} = 65$ mm. Maximum value 80,47 mm

The numerically obtained deflection modes for $h_{ini} = 86$ mm are illustrated in the next figures. The results indicate that the 2½-D model has lost its legitimacy.

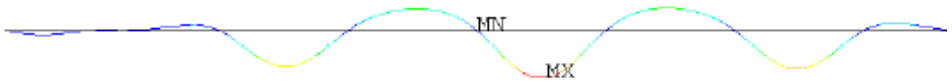


Figure 14: Plot of deflections IPE 300 girder 2-D model $h_{ini} = 86$ mm. Maximum value 233,97 mm

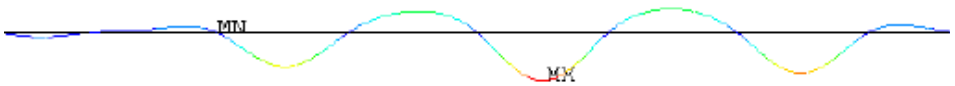


Figure 15: Plot of deflections IPE 300 girder 2½-D model $h_{ini} = 86$ mm. Maximum value 219,86 mm

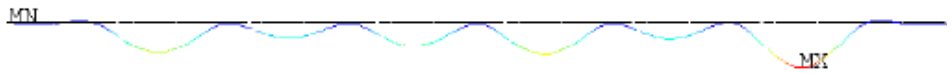


Figure 16: Plot of deflections IPE 300 girder 3-D model $h_{ini} = 86$ mm. Maximum value 107,54 mm

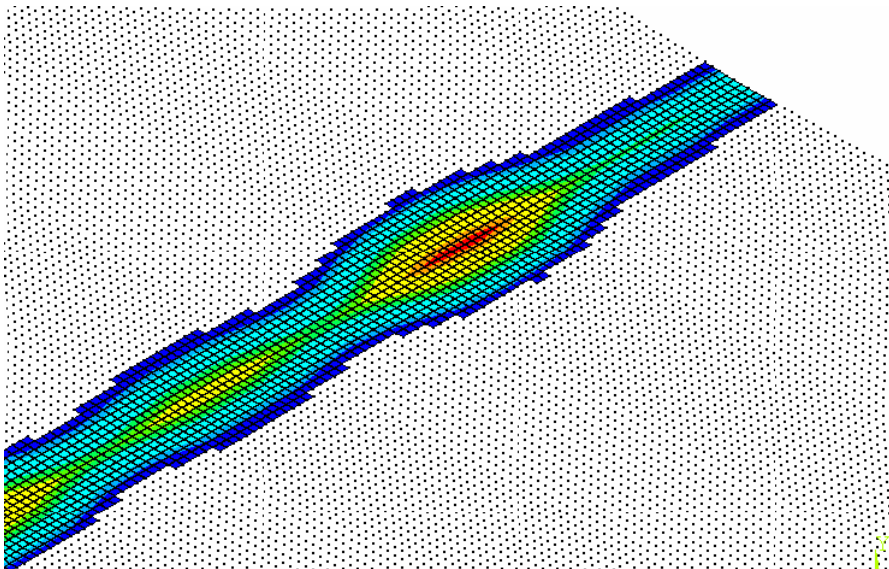


Figure 17: Contour plot of roof subjected to dead load and live load

The numerically determined water pressure with load factors above the girder IPE 300 in the second field (number axis 18 character axes B-C). The maximum water pressure occurs between character axes B and C .

Taking the three sets of figures into consideration it is lucidly demonstrated that only the 3-D model yields reliable results for all stated water elevations. Both other models produce valid results when the water front does not reach the model boundaries. The 3-D results point out that the collapse mechanism is not stability driven but strength (yield) driven.

In conclusion, it is necessary to utilize a 3-D model for sufficient, reliable and accurate solution of ponding problems. Apparently, 2-D and 2½-D model approaches may yield erroneous results. For matter of clarity a contour plot is inserted (Fig. 17) which represents the 3-D model water pressure distribution on the roof area above the IPE 300 girder for $h_{ini} = 65$ mm.

5 Conclusions

The major conclusions derived from the presented material can be stated as follows.

- Analytical solutions presented in literature sometimes neglect self-weight and thus only consider the ponding loads. However, this is an oversimplification of reality, and in such cases the presented solutions are more academic exercises than useful and fruitful methods for designing engineers.
- Analytical methods can only be developed for regular roof plans of orthogonal pattern. The ponding stability behaviour is different for each structure, which implies a strong path-dependency, which could most probably only be traced by numerical analysis. As a consequence the validity of analytical solution methods is rather limited.
- In order to avoid unsafe situations it should be underlined that the analytical solution methods lose their applicability for $n < 1$ due to the nonlinear stability response. Only very recently a theory was published to overcome this restriction (Blaauwendraad, 2007, Engineering Structures).
- The scatter of the safety factor is disproportionate and incalculable for model factor $\gamma_M = 1,3$. This typical behavior is also visible for model factor $\gamma_M = 1,1$.
- Analytical solution methods developed for simple two-way flat roof system can produce valid results only if they are cautiously applied. The risk of misjudgement is substantial.

- It is essential to employ a 3-D numerical model for sufficient, reliable and accurate solution of complicated ponding problems. Apparently, 2-D and 2½-D computational model approaches may yield erroneous results.

References

- Blaauwendraad, J. (2007) 'Ponding on Light-weight Flat Roofs: Strength and Stability' in *Engineering Structures*, Vol. 29, No. 5, pp. 832-849.
- Blaauwendraad, J. (2006) 'Ponding on flat roofs: A different perspective' in *HERON*, Vol. 51, No. 2/3, pp. 151-182.
- Colombi, P. (2006) 'The ponding problem on flat steel roof grids' in *Journal of Constructional Steel Research*, Nr. 62, pp. 647-655.
- Herwijnen van, F., H. H. Snijder and H. J. Fijneman (2006) 'Structural design for ponding of rainwater on roof structures' in *HERON*, Vol. 51, No. 2/3, pp. 115-150.
- Kool, E. J., W. P. P. Kolner and J. van der Meer (2003) *Instortingen van lichte platte daken Onderzoek*, VROM Inspectie.
- Marino, F. J. (1966) 'Ponding of Two-Way Roof Systems' in *AISC Engineering Journal*, July, pp. 93-100.